ACS Macro Letters

Letter

pubs.acs.org/macroletters

Dielectric Chain Dynamics of Side-Chain Liquid Crystalline Polymer

Yu Liu, Yaogong Li, and Huiming Xiong*

Department of Polymer Science, Shanghai Jiao Tong University, Shanghai, 200240, People's Republic of China

Supporting Information

ABSTRACT: Both chain dynamics and statistics of side-chain liquid crystalline polymer are experimentally explored. Dielectric measurements over a wide range of frequencies and temperature windows demonstrate that the chain dynamics in the liquid crystalline phase (SmA) is retarded and has higher apparent activation energy compared to that in isotropic melt. The molecular weight dependence of the normal mode relaxation time in the isotropic melt conforms to the Zimm model with excluded volume effect, while it shows Rouse behavior in the liquid crystalline phase. The mean squared end-to-end distance of polymer chain in the liquid crystalline phase decreases compared to that in the isotropic melt. The main chain takes a self-avoiding walk with $\langle R_e^2 \rangle \sim N^{2\nu}$, $\nu = 0.54-0.6$ in the isotropic melt, whereas a random walk between smectic layers with $\nu \cong 0.5$, consistent with the results from chain dynamics.

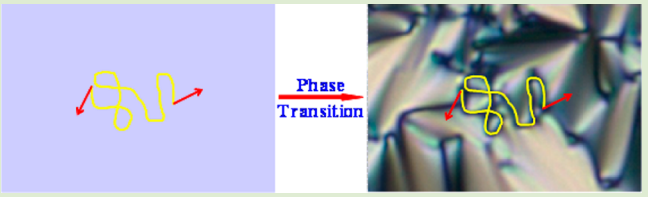

Thermotropic liquid crystals are interesting soft condensed materials due to combination of order and mobility compared to crystal and pure liquid. Side-chain liquid crystalline (SCLC) polymers, with liquid crystalline mesogens attached to the main chain, exhibit nontypical polymeric behaviors on the aspects of chain statistics and dynamics.[1−4] Although the classic theories of chain dynamics are successful, some mysteries of the global chain motion such as microscopic mechanism of chain friction remain elusive.[5−7] For SCLC polymers, the dynamics of main chain is expected to depend on details of chain structure, liquid crystalline field, monomeric friction coefficient, and so on. Therefore, the knowledge of the global chain dynamics of this anisotropic polymeric liquid, including how the intermolecular potential affects the chain statistics and the microscopic friction process, which relates to the temperature-dependence of chain dynamics on different length and time scales can deepen our understanding of polymer dynamics from a physical point of view of a chemically realistic model.

Investigation of chain dynamics in the liquid crystalline phase is technically challenging. One conventional technique to study chain dynamics is by rheological measurement. However, this method is tightly limited by the complex behaviors of liquid crystals linked to shear flow, macroscopic domains, defects evolution, and so on.[8] Dielectric relaxation spectroscopy, as another versatile tool, is capable of probing fluctuation of dipoles associated with various relaxation processes over a large frequency range. About five decades ago it was demonstrated that, when a polymer chain has a cumulative longitudinal dipole moment along its backbone, the global motion of this so-called type-A polymer could be reflected by its dielectric fluctuation of the end-to-end vector.[9] Meanwhile, the mean squared end-to-end distance of chains can be deduced from the dielectric strength, which is the most theories deal with in comparison to radius of gyration usually obtained through neutron scattering experiment with isotopic labeling.[10,11] In this Letter, we give the first experimental investigation on type-A SCLC polymers by using broadband dielectric spectroscopy and reveal how the presence of the liquid crystalline field can govern its chain dynamics and statistics. The quantitative differences of dynamics and statistics in different phases are discussed. We clearly demonstrate that the excluded volume effect exists in the isotropic melt, whereas Rouse behaviors are observed in the liquid crystalline phase.

Extensive research on local relaxation of SCLC polymers, for example, α-, β-, δ-relaxation and decoupling relaxation of mesogen from segmental relaxation of the main chain, have been previously conducted;[12−15] however, the nature of chain dynamics is far from being understood. One reason could be the ever availability of such type-A liquid crystalline polymer. In contrast to most SCLC polymers of flexible backbones based on polysiloxane, polydiene, and polymethacrylate, polyether, having a chemical structure of $-(CH_2-CHR\text{-}O)-$, is a typical type-A polymer.[16] Therefore, we designed and successfully synthesized a series of SCLC polyethers of different molecular weights by using an anionic polymerization. The samples are referred to as EOBCs. Their characteristics are listed in Table 1. Characterizations of their phase structures are shown in Figure 1 and Supporting Information. For EOBC3, as an example, it exhibits phase transitions from isotropic melt to SmA phase at 142.9 °C, SmA phase to a highly ordered (HO) phase at 72.2 °C, and a thermal glass transition around 7.2 °C. The considerable large phase temperature range enables investigation of relaxation processes as a function of temperature.

In dielectric spectroscopy of EOBC1 shown in Figure 2, a process appears around 0.6 MHz at 168 °C. It shifts gradually

Received: November 13, 2012
Accepted: December 17, 2012
Published: December 26, 2012

Table 1. Liquid Crystalline Polymers (EOBCs) Characteristics

sample	M_w (× 10^3) /DP[a,b]	PDI[b]	T_g (°C)[d]	$T_{HO\text{-}SmA}$ (°C)[d]	$T_{SmA\text{-}Iso}$ (°C)[d]	$E_{n\text{-}SmA}$ (kJ/mol)	$E_{n\text{-}Iso}$ (kJ/mol)	τ_{SmA}/τ_{Iso}[e]	$\langle Re^2\rangle_{SmA}^{1/2}$ (nm)[f]	$\langle Re^2\rangle_{Iso}^{1/2}$ (nm)[f]
EOBC1	12.6/34[c]	1.04	4.3	65.4	131.9	64.4	37.7	4.4	5.7	6.4
EOBC2	22.3/60[c]	1.01	6.1	70.1	138.6	62.3	38.4	5.6	6.9	9.2
EOBC3	52.6/140	1.1	7.2	72.2	142.9	62.9	38.5	7.5	11.6	15.1

[a]Static light scattering. [b]GPC. [c]MALDI-TOF. [d]DSC cooling at 10 °C/min. [e]136 °C. [f]PPG's values of dipole moment and length of one repeat unit along contour are used.

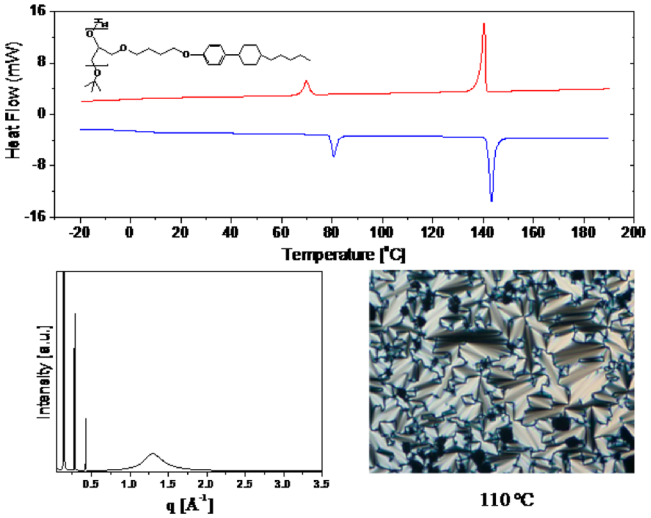

Figure 1. DSC diagrams of the representative sample EOBC3 at a rate of 10 °C/min; X-ray diffraction curve of EOBC3 in the SmA phase at 110 °C (bottom left) and its typical texture at 110 °C (bottom right). Inset is the chemical structure of EOBCs.

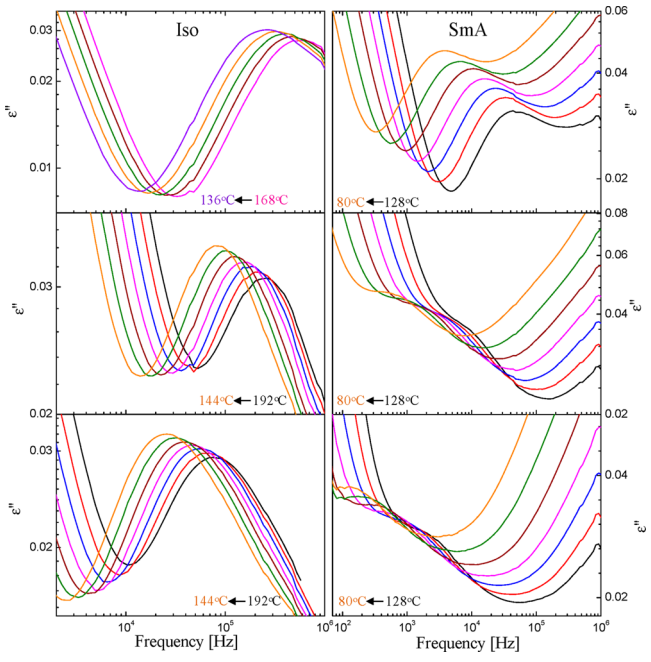

Figure 2. Representative dielectric spectra ε'' as a function of temperature at 8 °C step for EOBC1 (top), EOBC2 (middle), and EOBC3 (bottom). Left column: the isotropic melt; Right column: the SmA phase.

to lower frequency until 136 °C, where an abrupt change is observed with the relaxation peak shifting to lower frequency by about half a decade. Concurrently, there is another process that gradually moves into the frequency window. This sudden change of relaxation time is a signature of the phase transition from the isotropic melt to SmA phase, whose transition temperature agrees with that from differential scanning calorimetry (DSC) measurement. These dominant processes in the isotropic melt and SmA phase are observed in all EOBCs, which locate at correspondingly lower frequency with an increase in molecular weight. This apparent molecular weight dependence suggests that the process be a normal mode, a typical behavior of type-A polymer. The high frequency tail of the SmA phase is associated with local mode with negligible molecular weight dependence, which will be discussed in a future publication.

The complex dielectric permittivity ε^* can be well-fitted with one Havriliak–Negami (HN) function for the isotropic melt or two HN functions for the SmA phase in addition to a conductivity contribution, as shown below:

$$\varepsilon^* = \varepsilon_\infty + \frac{\Delta\varepsilon}{(1 + (i\omega\tau_{HN})^\beta)^\gamma} + i\frac{C}{\omega}$$

where τ_{HN} is the HN relaxation time; β and γ are the shape parameters of the HN function describing the symmetric and asymmetric broadenings of relaxation time distribution;[5,6] $\Delta\varepsilon$ denotes the relaxation strength; and C is directly related to the DC conductivity. We chose to focus on the maximum frequency ν_m of ε'', which depends on the parameter of β and γ via the following equation:

$$\nu_m = \frac{1}{2\pi\tau_{HN}}\left[\sin\frac{\beta\pi}{2+2\gamma}\right]^{1/\beta}\left[\sin\frac{\beta\gamma\pi}{2+2\gamma}\right]^{-1/\beta}$$

The processes of chain dynamics and α relaxation are well separated, which allows to resolve the peak position defining the time scale with low uncertainty, and reliable ν_m data in the entire experimental temperature range can be obtained after simultaneous fitting to the real and imaginary parts of ε^*. Arrhenius plot of ν_m as a function of reciprocal temperature for EOBCs in the isotropic melt and SmA phase are shown in Figure 3. As is known, when the temperature is approaching the glass transition temperature, the activation energy could be temperature-dependent for fragile materials, which leads to non-Arrhenius behavior.[17] However, for our case, Arrhenius law can yield a satisfactory description of the temperature-dependence of ν_m, at least in the measured temperature window, including the smectic phase temperature range, which enables us to compare the apparent activation energies in different phases. It is also found that there is no apparent molecular weight dependence of apparent activation energies for the isotropic melt and SmA phase, which are $E_{n\text{-}Iso} \sim 38$ kJ/mol and $E_{n\text{-}SmA} \sim 63$ kJ/mol. Because of that, we chose to compare the chain relaxation time $\tau_n = 1/2\pi\nu_m$ at a temperature of 136 °C. Although this temperature may not necessarily coincide with the real phase transition temperatures of all the

dx.doi.org/10.1021/mz3005988 | ACS Macro Lett. 2013, 2, 45–48

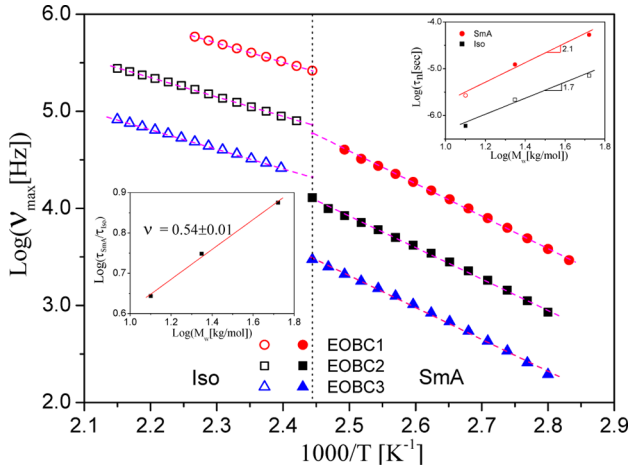

Figure 3. Arrhenius plots of peak relaxation rates ν_m vs reciprocal temperature for EOBCs in the isotropic melt and SmA phase. The lines represent Arrhenius fits. The upper right inset is the relationship of τ_n with M_w of EOBCs in the isotropic melt and SmA phase at 136 °C. The open symbols in the inset are the data points obtained by extrapolation of Arrhenius fits to 136 °C. The fits to the power law give the exponents of 2.1 and 1.7, with the uncertainties within 0.2. The lower left inset is the double logarithmic plot of (τ_{SmA}/τ_{Iso}) vs M_w of EOBCs. The linear fitting yields $\nu = 0.54 \pm 0.01$.

samples observed in dielectric experiments, it is rather close to either phase, as illustrated in Figure 3.

Dielectric normal mode relaxation spectrum is dominated by the slowest chain modes. For a Rouse chain, $\tau_p = \tau_0\pi^2/(4\sin^2(p\pi/2N))$, $p = (0, 1, ..., N-1)$, $\tau_0 = b^2\xi/3\pi^2k_BT$, b is the effective Rouse segment length or dynamic bead size, ξ is the friction coefficient of a bead, N is the number of bead. The peak frequency of dielectric normal mode provides a rather direct access to the longest Rouse time of the smallest p, where $\tau_n \cong \tau_1 \cong \xi N^2b^2/3\pi^2k_BT$ holds. Because N is proportional to the molecular weight, M_w, Rouse model predicts $\tau_n \propto M_w^2$. When hydrodynamic interaction is taken into account, especially in polymer solution, the Zimm model achieves a great success. It predicts $\tau_n \cong \tau_1 \cong \eta_s N^{3\nu}b^3/k_BT$.[18] The exponent ν is 1/2 in θ solvent and ~3/5 in a good solvent, the same as the Flory exponent in the static scaling. For EOBCs in isotropic melt and SmA phase, the chain relaxation times τ_n at 136 °C are plotted versus molecular weight, and fits of $\tau_n \propto M_w^{1.7}$ for the isotropic melt, and $\tau_n \propto M_w^{2.1}$ for the SmA phase are obtained, as demonstrated in the upper right inset of Figure 3. These scaling laws suggest that the chain dynamics in the isotropic melt conforms to the Zimm model for excluded volume chain, whereas the chain dynamics in the SmA phase exhibits Rouse behavior.

By passing the phase transition temperature from the isotropic melt to the SmA phase, the chain motion slows down, as shown in Figure 3, accompanying with reduction in dielectric strength and broadening of the peak with change of shape parameter $\gamma \sim 0.6$ in the isotropic melt to ~0.4 in the SmA phase, while β keeps close to 1. The ratio of chain relaxation time in the SmA phase (τ_{SmA}) to that in the isotropic melt (τ_{Iso}) at 136 °C, τ_{SmA}/τ_{Iso}, increases with an increase in molecular weight, as given in Table 1. The apparent molecular weight dependence of τ_{SmA}/τ_{Iso} suggests that the chain dynamics in the isotropic melt and SmA phase should have different scaling laws with molecular weight. If the Zimm model $\tau_{Iso} \propto N_{Iso}^{3\nu}$ in the isotropic melt and Rouse dynamics $\tau_{SmA} \propto N_{SmA}^2$ in the SmA phase are taken, the ratio of (τ_{SmA}/τ_{Iso}) for polymers of different molecular weights M_w should scale with M_w as $M_w^{2-3\nu}$. The lower left inset of Figure 3 shows the double logarithmic plot of (τ_{SmA}/τ_{Iso}) versus M_w. The linear fitting gives the exponent $\nu = 0.54 \pm 0.01$. The value of exponent ν is also consistent with the static scaling law of chain dimension with molecular weight, as demonstrated later. This is strong evidence that the polymer chains are subjected to excluded volume interaction in the isotropic melt, while it is screened in the SmA phase. It is rather surprising to see the Rouse behaviors in the liquid crystalline phase, whereas excluded volume effect in the isotropic melt. These results thus emphasize that the details of chain structure as well as the liquid crystalline ordering are playing important roles and these characters are not captured by classic Rouse−Zimm models.

Compared to other methods, broadband dielectric spectroscopy has an advantage that it can not only probe the characteristic chain relaxation time, but also its statistics, derived through relaxation strength.[5,6,19,20] Because the static correlation of the end-to-end vector among different polymer chains can be neglected, Onsager equation is applicable to the normal modes of EOBCs in the isotropic melt and SmA phase.[21] The relaxation strength of the normal mode $\Delta\varepsilon_n$ is expressed in the MKS unit as

$$\Delta\varepsilon_n = \frac{3(\Delta\varepsilon_n + \varepsilon_s)}{2\Delta\varepsilon_n + 3\varepsilon_s}\cdot\frac{(\varepsilon_s + 2)^2}{9}\cdot\frac{\rho\mu^2N_A}{3M_wl^2\varepsilon_0k_BT}\cdot\left\langle R_e^2\right\rangle$$

where $\Delta\varepsilon_n = (\varepsilon_n - \varepsilon_s)$, ε_n, ε_s are the plateau values of the real part of the complex dielectric function at the low and high frequency side of the normal mode, whereas the former corresponds to the static permittivity of normal mode, the latter corresponds to the static permittivity for segmental relaxation; ρ is the density, whose room temperature value of 0.989 g/cm^3 is used; μ is the magnitude of monomeric dipole moment along the chain contour; l is the length of monomer; R_e is the end-to-end distance of the chain; k_B is the Boltzmann constant; ε_0 is the permittivity of vacuum; N_A is the Avogadro constant. Therefore, $\langle R_e^2\rangle$ can be calculated with knowledge of μ and l. The values 0.18 D (D: Debye unit) and 3.58 Å of poly(propylene glycol) (PPG) are chosen for the sake of simplicity.[22] Nevertheless, the absolute value will not have any effect on the discussion in this Letter.

The statistics of polymer main chain in different phases are thus obtained. The temperature dependences of $\langle R_e^2\rangle^{1/2}$ of EOBCs in the isotropic melt and SmA phase are shown in Figure 4. When phase transition from the isotropic melt to SmA phase takes place, decrease of $\langle R_e^2\rangle^{1/2}$ is clearly observed for all the samples. One way to describe chain statistics of a polymer is to establish the relation between the chain dimension to its molecular weight, $\langle R_e^2\rangle \sim N^{2\nu}$, ν is the Flory exponent, depending on the nature of the walk adopted by the polymer. The average $\langle R_e^2\rangle$ of EOBCs in the different phase temperature ranges are thus plotted as the function of molecular weight in the inset of Figure 4. The linear fittings give estimations of ν ~0.6 in the isotropic melt and ~0.5 in the SmA phase. These values agree well with the scaling laws of chain relaxation time with molecular weight, as shown in the inset of Figure 3. These results strongly suggest that the polymer chain does take a self-avoiding walk in the isotropic melt, while is Gaussian in the SmA phase.

For SCLC polymers, there exists a competition between entropy of polymer backbone maximized by adopting a random

dx.doi.org/10.1021/mz3005988 | ACS Macro Lett. 2013, 2, 45−48

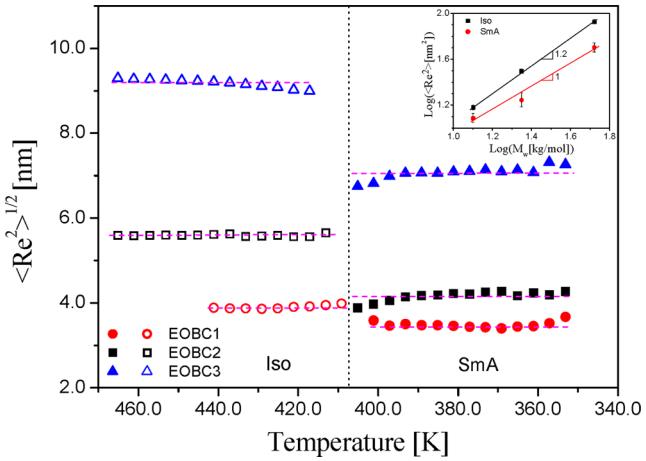

Figure 4. Temperature dependence of root mean squared end-to-end distance ($\langle R_e^2\rangle^{1/2}$) of EOBCs in the isotropic melt and SmA phase. Dashed lines are guides for eyes. Inset is the double logarithmic plots of average $\langle R_e^2\rangle$ vs M_w in the isotropic melt and SmA phase.

coil conformation, and orientational ordering of liquid crystalline mesogen. In the SmA phase, polymer backbone is distributed preferentially between liquid crystalline layers due to microsegregation between the main chain and mesogenic groups.[23] The X-ray results of EOBCs also indicate that the polymer backbone is mainly confined between smectic layers. Based on dielectric measurement, the larger $\langle R_e^2\rangle$ obtained in the isotropic melt than that in the SmA phase can be caused by diluent effect of side groups in the isotropic melt;[11] in the SmA phase, better ordering of side mesogenic groups leads to the decrease of the dimension of the main chain. This is also consistent with the picture that the chains are excluded in the isotropic melt while screened in the SmA phase. The pendent groups in this case may serve as solvent in the isotropic melt, leading to self-avoiding walk of the main chain.

It is interesting to find that these two types of chain walks have different apparent activation energies, which are $E_{\text{n-Iso}} \sim 38$ kJ/mol and $E_{\text{n-SmA}} \sim 63$ kJ/mol, respectively. In the isotropic melt, the temperature dependence of chain dynamics can be primarily controlled by the flow activation energy at such high temperature Arrhenius region (>140 °C + T_g).[24] When EOBCs go into the liquid crystalline phase, the chain relaxation time increases a few times and the apparent activation energy increases ~1.7 times; the chain dynamics in the liquid crystalline phase shows a typical Rouse behavior. It is known that for a bead−spring Rouse chain, the temperature dependence of chain dynamics originates mainly from temperature dependence of friction coefficient of the bead. Traditionally, it is assumed to be the same as monomeric friction coefficient which also controls segmental relaxation. In liquid crystalline phase, the motion of polymer main chain is necessarily involved in rearrangement of the backbone together with translational motion of mesogens in fluidic smectic layers. The chain will feel the friction contributed by interaction among the pendent liquid crystalline mesogen groups, which results in higher apparent activation energy than that in the isotropic melt and also slows down the chain dynamics. A theory describing SCLC polymer chain dynamics and statistics coupled with liquid crystalline field is called for.

■ ASSOCIATED CONTENT

Supporting Information

Characterization by using MALDI-TOF mass spectrum, 2D WAXD, and dielectric measurements. This material is available free of charge via the Internet at http://pubs.acs.org.

■ AUTHOR INFORMATION

Corresponding Author

*E-mail: hmxiong@sjtu.edu.cn.

Notes

The authors declare no competing financial interest.

■ ACKNOWLEDGMENTS

X.H.M. appreciates Dr. M. Nakanishi for assistance with dielectric measurement and helpful discussion. We acknowledge CFN and NSLS (X9 beamline) at BNL, BL16B, and BL14B in SSRF and A. P. Sokolov for use of their facilities. Research is supported by the NSFC (No. 21074070), NCET-11-0335, Shanghai Pujiang Program (10PJ1405400), and Research Fund for the Doctoral Program of Higher Education (20100073110027).

■ REFERENCES

(1) Finkelmann, H.; Ringsdorf, H.; Wendorff, J. H. *Makromol. Chem.* **1978**, *179*, 273.
(2) Shibaev, V. P.; Platé, N.; Freidzon, Y. S. *J. Polym. Sci., Polym. Chem. Ed.* **1979**, *17*, 1655.
(3) Warner, M. In *Side Chain Liquid Crystal Polymers*; McArdle, C. B., Ed.; Blackie: London, 1989; Chapter 2.
(4) Wang, R.; Wang, Z. G. *Macromolecules* **2010**, *43*, 10096.
(5) Sokolov, A. P.; Schweizer, K. S. *Phys. Rev. Lett.* **2009**, *102*, 248301.
(6) Ngai, K. L.; Plazek, D. J.; Roland, C. M. *Phys. Rev. Lett.* **2009**, *103*, 159801.
(7) Sokolov, A. P.; Schweizer, K. S. *Phys. Rev. Lett.* **2009**, *103*, 159802.
(8) Schneider, F.; Kneppe, H. In *Handbook of Liquid Crystals*; Demus, D., Goodby, J., Gray, G. W., Spiess, H.-W., Eds.; Wiley-VCH Verlag GmgH: New York, 1998; Vols. *V, VIII*.
(9) Stockmayer, W. H. *Pure Appl. Chem.* **1967**, *15*, 539.
(10) Cotton, J. P.; Hardouin, F. *Prog. Polym. Sci.* **1997**, *22*, 795.
(11) Noirez, L.; Boeffel, C.; Daoud-Aladine, A. *Phys. Rev. Lett.* **1998**, *80*, 1453.
(12) Kremer, F., Schönhals, A., Eds. *Broadband Dielectric Spectroscopy*; Springer: New York, 2003.
(13) Runt, J., Fitzgerald, J., Eds. *Dielectric Spectroscopy of Polymeric Materials*; ACS Books: Washington, DC, 1997.
(14) Schick, C.; Sukhorukov, D.; Schönhals, A. *Macromol. Chem. Phys.* **2001**, *202*, 1398.
(15) Elmahdy, M. M.; Floudas, G.; Oldridge, L.; Grimsdale, A.; Müllen, K. *ChemPhysChem* **2006**, *7*, 1431.
(16) Baur, M. E.; Stockmayer, W. H. *J. Chem. Phys.* **1965**, *43*, 4319.
(17) Angell, C. A. *J. Non-Cryst. Solids* **1991**, *131−133*, 13.
(18) Doi, M.; Edwards, S. F. *The Theory of Polymer Dynamics*; Clarendon: Oxford, U.K., 1986.
(19) Zimm, B. H. *J. Chem. Phys.* **1956**, *24*, 269.
(20) Adachi, K.; Kotaka, T. *Prog. Polym. Sci.* **1993**, *18*, 585.
(21) Onsager, L. *J. Am. Chem. Soc.* **1936**, *58*, 1486.
(22) Stockmayer, W. H. *Pure Appl. Chem.* **1967**, *15*, 539.
(23) Lipatov, Y. S.; Tsukruk, V. V.; Shilov, V. V. *Polym. Commun.* **1983**, *24*, 75.
(24) Ferry, J. D. *Viscoelastic Properties of Polymers*, 3rd ed.; Wiley: New York, 1980.